



Research Article

The Effect of Filament Materials (Tungsten, Lanthanum Hexaboride) in 250 keV/1 mA Electron Beam Machines on Empirical Capacity of RVNRL

Herry Poernomo¹, Suhadah Rabi'atul Adabiah^{2,*}, Darsono Darsono², Suprpto Suprpto²,
Djoko Slamet Pudjorahardjo², Samin Samin¹, Kris Tri Basuki¹

¹Research Center for Mining Technology, Research Organization for Nanotechnology and Materials, National Research and Innovation Agency (BRIN), Puspitpek Area, KST B.J. Habibie, Tangerang Selatan, Banten, 15314, Indonesia

²Research Center for Accelerator Technology, Research Organization for Nuclear Energy, National Research and Innovation Agency (BRIN), Puspitpek Area, KST B.J. Habibie, Tangerang Selatan, Banten, 15314, Indonesia

*Corresponding author: suha036@brin.go.id

Abstract: Some types of filaments sold commercially are made of tungsten and a lanthanum hexaboride (LaB₆) with a lifetime of approximately 30-100 hours and > 1000 hours, respectively. The lifetime of filament significantly affects the effective operation time of one year on Electron Beam Machines (EBM) used for the vulcanization of natural rubber latex. Therefore, this study aimed to empirically determine the Radiation Vulcanized Natural Rubber Latex (RVNRL) capacity using one EBM unit with electron gun made of tungsten filament or LaB₆ at maximum and safe operating conditions (e-beam energy, $E = 250$ keV, e-beam current, $I = 1$ mA, and the distance from the window to the NRL film, $t_a = 3$ cm). RVNRL capacity was determined using empirical equation containing several process condition variables and EBM technical specifications. The results showed that using tungsten or LaB₆ as materials for filament produced RVNRL capacity of 20.22 tons/year or 36.92 tons/year, respectively. This showed that empirical calculation of RVNRL capacity could be used to determine the amount of EBM at a certain RVNRL production level.

Keywords: Electron beam machines; Filament; Lanthanum hexaboride; RVNRL; Tungsten

1. Introduction

Natural rubber latex (NRL) is a milky white biopolymer latex derived from *Hevea brasiliensis* Muel.Arg. The NR molecule consists of cross-linked isoprene units that form a cis-1,4 polyisoprene structure (Baudoin et al., 2025; Lonartz et al. 2023; Andrade et al., 2022; Lehman et al., 2022; Yamano et al., 2021; Andler, 2020; Kim et al., 2020; Cifriadi et al., 2017; Junkong et al., 2017; Harahap et al., 2015; Singh et al., 2015; Che et al., 2013; Tosaka et al., 2006; Trabelsi et al., 2004). Based on statistical data in 2019, World natural rubber (NR) production was 13,804 million tonnes, which would increase by 2.7% annually (Muktariidha et al., 2021). Vulcanized natural rubber latex (VNRL) with sulfur, contains carcinogenic compounds such as N-nitroso morpholine, 4-nitroso morphine, and dimethylnitrosamine, which in parts per billion (ppb) can cause cancer (Li and Hecht, 2022; Li et al., 2021; Widiyati and Poernomo, 2018; Radford et al., 2013).

This work was supported by the Research Organization for Nuclear Energy, National Research and Innovation Agency (BRIN), funded by DIPA ORTN BRIN Grant No. 6691.SDB.001.051E (2022).

<https://doi.org/10.14716/ijtech.v16i4.6475>

Received May 2023; Revised August 2023; Accepted October 2023

The cross-linking process using irradiation has numerous advantages and can be applied to improve materials performance (Febriasari, et al., 2021). Specifically, the cross-linking of polyisoprene in RVNRL process is stronger compared to VNRL process with sulfur. In RVNRL, there is a direct cross-linking between carbon atoms without going through a sulfur atom with a bond energy of around 58.6 kcal/mol. This C-C bond is a significantly larger carbon-sulfur bond energy of approximately 27.5 kcal/mol (Marsonkho, 2013).

Filament materials that are widely used as electron sources in Electron Beam Machines (EBM), Scanning Electron Microscope (SEM) analysis equipment, and Electron Microscope Transmission (TEM) are tungsten and LaB₆. The raw materials for making LaB₆ is lanthanum oxide (La₂O₃), which is a light rare earth oxide (LREO) (Trisnawati et al., 2020; Samin et al., 2020). Moreover, the lifetime of tungsten and LaB₆ filament is 30-100 hours and > 1000 hours, respectively, as shown in Table 1 (EMS, 2023; Poernomo and Saptaji, 2012).

Table 1 Characteristics of LaB₆, CeB₆, and Tungsten filaments

Parameter	LaB ₆	CeB ₆	Tungsten
Brightness (A cm ⁻² sr ⁻¹)	10 ⁷	10 ⁷	10 ⁶
Short-term beam current stability (%RMS)	< 1	< 1	< 1
Typical service life (hr)	1000+	1500+	30-100
Operating vacuum (torr)	10 ⁻⁷	10 ⁻⁷	10 ⁻⁵
Work function (eV)	~	~	4.5
Evaporation rate (g cm ⁻² sec ⁻¹)	2.2x10 ⁻⁹	1.6x10 ⁻⁹	

One of the existing low-energy tungsten filament-based EBMs in Indonesia was specifically designed for RVNRL process. The design specifications included electron beam energy $E = 300$ keV, electron beam current $I = 20$ mA, window size (width $s = 6$ cm, length $L = 60$ cm), Ti window foil thickness $t_w = 20$ μ m, absorbed dose $D = 50$ kGy (Darsono et al., 2024; Darsono, 2009).

EBM performance has been tested with initial design specifications of 300 keV/20 mA by measuring the maximum voltage and current that can be achieved under safe EBM operating conditions. The output electron beam energy and current that can be safely achieved are $E = 250$ keV and $I = 1$ mA, respectively (Sukaryono, 2021). The EBM that has been tested under safe conditions with a maximum operating condition of 250 keV/1 mA is shown in Figure 1 (Darsono, 2009; Suprpto and Djoko, 2007).

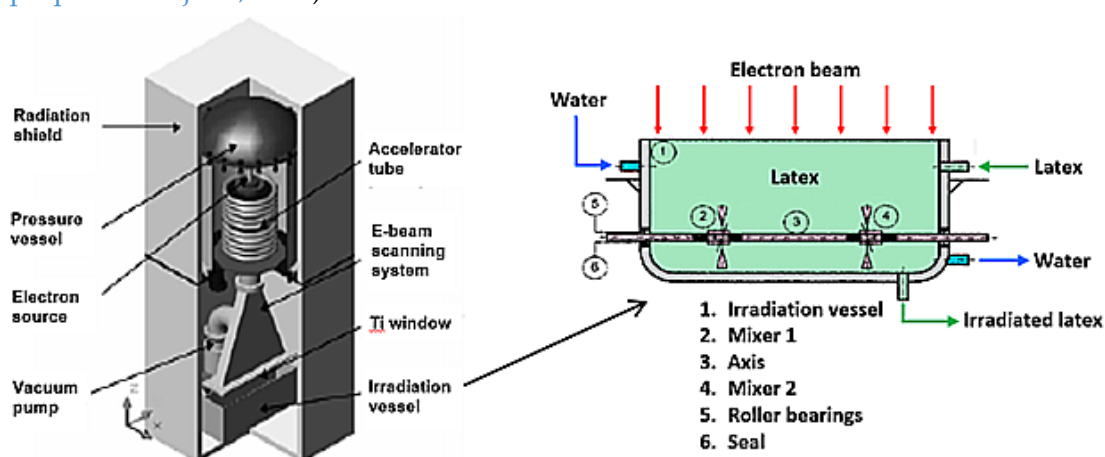


Figure 1 The EBM for RVNRL at maximum operational test conditions of 250 keV/1 mA

The irradiation vessel system presented in Figure 1 has weaknesses, including:

- The top NRL thin layer irradiated with electron beam will receive a repeated bombardment of electron beam, which causes the NRL to become hot and leads to NRL degradation.

- During stirring, the foam may form in the NRL. The froth can reduce the quality of irradiated latex because most of the e-beam will be absorbed by the foam that appears, reducing the cross-linking process of isoprene in NRL to poly-isoprene.

- The rubber seals on the stirrer rotor interact with chemical reactants such as n-BA, KOH, and ammonia in NRL. This interaction can accelerate damage to the rubber seals, causing NRL leakage from the irradiation vessel.

A solution has been identified to address the problem of irradiated NRL degradation due to the influence of the long irradiation time and temperature that arises in RVNRL process, as shown in Figure 1. This includes shooting the NRL film on a conveyor belt with electron beam from EBM at a certain speed and a maximum distance of 3 cm, as shown in Figure 2 (Kovalskiy, 2017).

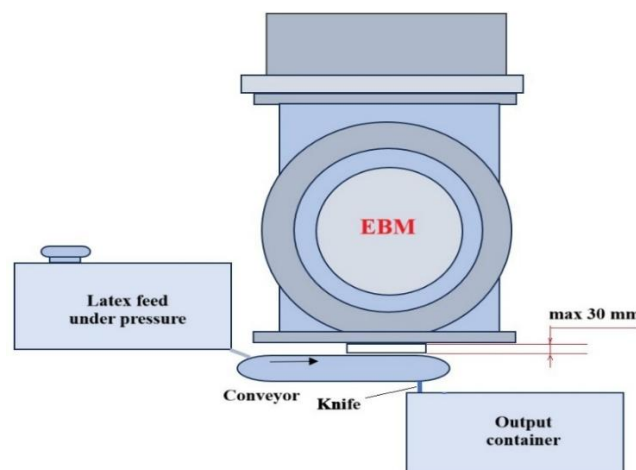


Figure 2 EBM 200 keV/26 A of prototype based on e-beam from plasma cathode for RVNRL process using belt conveyor

The maximum window distance to the surface of the NRL film, which is irradiated with electron beam produced from EBM with specifications of 200 keV/26 A is $t_a = 3$ cm, as shown in Figure 2. The condition $t_a = 3$ cm is used as a database to determine the effect of $t_a = 1, 2, 3, 4$, and 5 cm on RVNRL capacity using EBM 250 keV/1 mA.

RVNRL capacity is an important characteristic that can be used to determine the number and the specifications of EBM required in calculating the capital investment plan. Moreover, the determination of RVNRL capacity can be carried out from several empirical equations that are affected by numerous variables such as EBM data characteristics, chemical and physical properties of latex, and other operating conditions.

The difference in the service life of tungsten filament and LaB_6 in EBM can affect the amount of NRL irradiated by electron beam per unit time, which is expressed by RVNRL capacity. Moreover, the novelty of this study is to determine the effect of tungsten and LaB_6 as electron sources in EBM irradiator with 250 keV/1 mA on RVNRL capacity. This is an important parameter to determine the performance of the EBM irradiator. The purpose of this study was to compare these two types of filament materials as electron source in the EBM irradiator based on RVNRL capacity calculation results from empirical equation with the maximum EBM operating conditions of 250 keV/1 mA. The results were expected to serve as input data for the potential users to determine the number of EBM that could be used for RVNRL plant's production capacity design in Indonesia.

2. Methods

2.1. Determining electron beam penetration before passing window foil

The determination of electron beam penetration is carried out to assess the depth in material. Specifically, electron beam penetration is a dose control parameter in irradiating a material to ensure uniform absorption and maintain homogeneous quality. In this context, the relative dose

compares the value absorbed during irradiation to the maximum dose. The reach of electron beam produced by filament as electron source in the EBM (R , g/cm²) is expressed by the following equation (Saptaaji, 2008):

$$R = 0,412 \times E^n \quad (1)$$

with, E = electron beam energy (MeV). Under conditions: $0.01 < E < 2.5$ MeV, then the n is determined by:

$$n = 1,265 - 0,094 \ln E \quad (2)$$

The energy absorbed in material has an uneven distribution, showing that the power absorbed per volume unit is a distance function. Empirically, beam power absorbed by the unit volume p_A at a distance z is expressed as follows (Saptaaji, 2008):

$$P_A/P_{Amax} = 1 - 9/4 \left(\frac{z}{R} - \frac{1}{3} \right)^2 \quad (3)$$

where p_{Amax} is the maximum value of absorption power per unit volume at electron penetration z of $R/3$ on the surface, z is penetration of electron beam generated by filament as a source of EBM electron ranging from 0 g/cm² to (R , g/cm²) at conditions of E .

2.2. Determining electron beam penetration after passing window foil

Heat accumulation occurred in the NRL film when applied with electron beam causing water evaporation. The water vapor on the surface of the NRL film affected the penetration of electron beam. Moreover, the amount of electron beam penetration after passing through the window and the air gap (P_1) could be determined using the equation:

$$P_1 = P_0 - [(t_w \times \rho_w) + (t_a \times \rho_a)] \quad (4)$$

with, P_0 = penetration of electron beam before passing through the window (g/cm²), t_w = window foil thickness (cm), ρ_w = window foil density (g/cm³), t_a = air gap thickness containing water vapor in the top of the NRL film (cm), and ρ_a = the density of air (g/cm³).

Electron beam that penetrates the NRL is backscattered, ionized, and excited. Subsequently, as a technical factor, the penetration of electron beam is taken = $0.9 \times P_0$ and equation (4) becomes (Poernomo and Saptaaji, 2012):

$$P_2 = 0.9 \times P_0 - [(t_w \times \rho_w) + (t_a \times \rho_a)] \quad (5)$$

2.3. The maximum thickness of NRL film that can be penetrated by electron beam

The amount of electron beam penetration after passing through the window, the air gap, and the NRL film can be determined using the equation (Poernomo and Saptaaji, 2012):

$$P_3 = 0.9 \times P_0 - [(t_w \times \rho_w) + (t_a \times \rho_a) + (t_l \times \rho_l)] \quad (6)$$

with, t_l = thick thin layer of latex (cm), ρ_l = latex density (g/cm³).

The ideal penetration of electron beam on the NRL film is when all electron beam can penetrate and interact with the NRL, with $P_3 = 0$.

$$0 = 0.9 \times P_0 - [(t_w \times \rho_w) + (t_a \times \rho_a) + (t_l \times \rho_l)] \quad (7)$$

From equation (7), the thickness of the NRL film that can be penetrated by electron beam (t_l) is determined using the equation (Widiyati and Poernomo, 2022):

$$t_l = [0.9 \times P_0 - [(t_w \times \rho_w) + (t_a \times \rho_a)]] / \rho_l \quad (8)$$

2.4. Calculating RVNRL capacity

The correlation between velocity v (m/sec) materials irradiated with electron beam energy E (MeV), beam current I (mA), the efficiency factor η (%), penetration of electron beam in material P_t (g/cm²), absorbed dose D (kGy or kJ/kg or kW.sec/kg), wide of scanning horn, s (m), was explained in the following equation (IAEA, 2010):

$$v = (E \times I \times \eta) / (10 \times P_i \times D \times s) \quad (9)$$

The flow rate of the RNL film above the irradiated belt conveyor (Widiyati and Poernomo, 2022; 2018)

$$F = v \times A \quad (10)$$

With, F = flow rate in the NRL films on the belt conveyor (cm³/sec), A = area of NRL film with the thickness as electron beam penetration (cm²). Consequently, the rate of latex film corresponding to electron beam penetration is as follows:

$$F = v \times (t_l \times L) \quad (11)$$

With, L = the window length (cm). Capacity of RVNRL (C , g/sec) is as follows:

$$C = F \times \rho_l \quad (12)$$

3. Results and Discussion

3.1. RVNRL uses EBM with a continuous electron beam from filament-based electron source of tungsten or LaB₆ materials

RVNRL production process uses 330 days or 7920 hours of operation, with a tungsten filament lifetime of 100 hours, requiring replacement approximately 79 times/year. Using LaB₆ filament with a lifetime of 1000 hours, the replacement is approximately 8 times per year. Each time the start-up is re-conducted in EBM filament post-replacement, achieving the desired vacuum condition requires a vacuum pump operation time of approximately 2 hours. Additionally, the window foil needs replacement during the continuous operation of the EBM. It is predicted that every time replacements of filament, window foil, and re-conditioning in the vacuum system requires a total time of 2 days:

- The number of effective days in one operational process year of RVNRL = 330 – (2 × 79) = 172 days (using tungsten filament).
- The number of effective days in one operational process year of RVNRL = 330 – (2 × 8) = 314 days (using LaB₆ filament).

3.2. The results of calculations of electron beam penetration (P_o) before window foil on filament-based EBM

The dose distribution of electron beam penetration in the NRL film is needed to determine penetration depth. By using equations (1) and (2) at an energy of 0.250 MeV, the value of R is 0.059 g/cm². With electron beam penetration (z) starting at 0 g/cm² to 0.05 g/cm², p_A/p_{Amax} can be obtained from equation (3). Electron beam penetration is a key dose control parameter for irradiating materials to ensure homogeneity and maintain irradiation quality. This results in $p_A/p_{Amax} = D/D_{max}$, where $D_{relative} = D/D_{max}$ represents the relative dose. The relative dose is the ratio of the absorbed dose during irradiation to the maximum dose. Moreover, the correlation of z with $D_{relative}$ obtained in this study is shown in Table 2.

Table 2 Correlation of z to $D_{relative}$

z (g/cm ²)	$D_{relative}$
0.000	0.750
0.010	0.938
0.020	1.000
0.030	0.935
0.040	0.742
0.050	0.423

From Table 2, the curve of relative dose distribution ($D_{relative}$) vs. electron beam penetration (z) can be constructed, as shown in Figure 3, with $D/D_{max} = D_{relative}$.

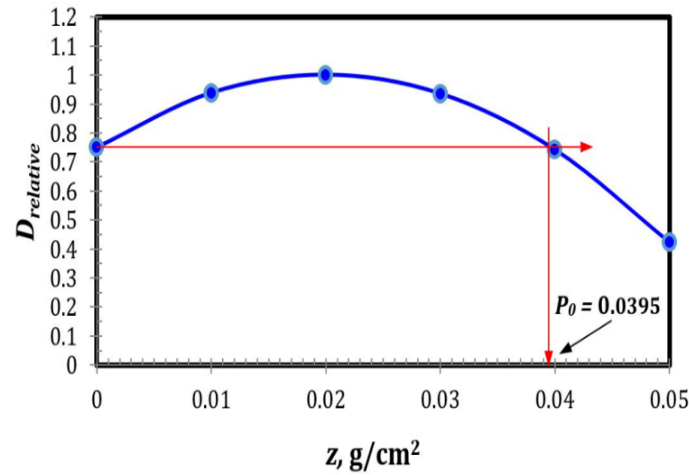


Figure 3 $D_{relative}$ vs. z at maximum operation condition EBM of 250 keV/1 mA

The determination of P_o was carried out at electron beam energy of 250 keV. At $D_{relative} = 0.75$, a straight line is drawn to cut the curve. Subsequently, a straight line is drawn from the point of intersection to intersect the abscissa of z on the points P_o of 0.0395 g/cm².

3.3. The results of calculations of RVNRL capacity using EBM with filament-based electron sources

Empirical calculation of RVNRL capacity on EBM under safe operating conditions 250 keV/1 mA for tungsten and LaB₆ are 172 effective days/year and 314 effective days/year, respectively. Based on data such as $E = 250$ keV, $I = 1$ mA, $s = 6$ cm, $L = 60$ cm, $D = 50$ kGy, $\eta = 60\%$, $\rho_a = 0.00112$ g/cm³, $\rho_l = 0.913$ g/cm³, $t_w = 20$ μ m, and $\rho_w = 4.6$ g/cm³, the effect of t_a and C can be determined using equations (4), (8), (9), (11), and (12), as shown in Figure 4.

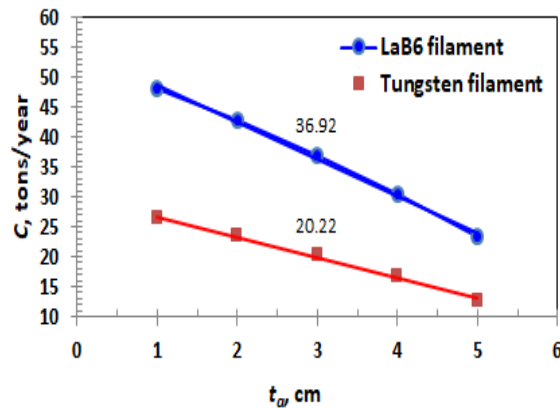


Figure 4 The effect of t_a and EBM filament materials on the C for EBM operates at $E = 250$ keV, $I = 1$ mA, and $D = 50$ kGy

The selection of distance from the window to the NRL film (t_a) in the EBM operation is 250 keV/1 mA. This is safely adopted from the operating conditions of the plasma cathode-based EBM, which has been successfully tested in Russia for RVNRL process with $t_a = 3$ cm, as shown in Figure 2 (Kovalskiy, 2017). Based on data such as $E = 250$ keV, $s = 6$ cm, $L = 60$ cm, $D = 50$ kGy, $\eta = 60\%$, $\rho_a = 0.00112$ g/cm³, $\rho_l = 0.913$ g/cm³, $t_a = 3$ cm, $t_w = 20$ μ m, $\rho_w = 4.6$ g/cm³, the effect of I and C can be determined from equations (4), (8), (9), (11), and (12), as shown in Figure 5.

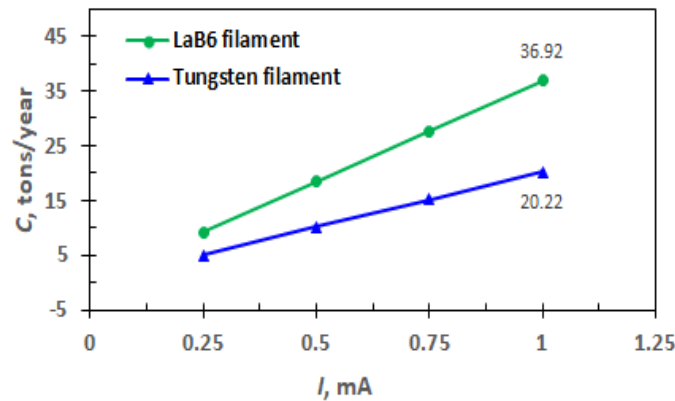


Figure 5 The effect of I and EBM filament materials on the C for EBM operates at $E = 250$ keV, $t_a = 3$ cm, and $D = 50$ kGy

Figure 5 demonstrates that higher electron beam current increases RVNRL capacity, which is crucial for maintaining performance during EBM operation. With greater electron beam current, the linear speed of NRL on the conveyor belt increases, leading to higher RVNRL capacity. Using a tungsten filament under optimal EBM conditions (at $E = 250$ keV, $I = 1$ mA, and $t_a = 3$ cm) results in a capacity of 18.70 tons/year, while using LaB₆ increases it to 34.15 tons/year.

The results of the absorbed dose calculation on the development of 250 keV and 300 keV filament EBM in Japan for each RVNRL process resulted in $D = 168$ kGy and 81 kGy, respectively (Poernomo and Saptaaji, 2012). This showed that EBM based on tungsten filament or LaB₆ could operate safely at a maximum condition of 250 keV/1 mA and adjusted the absorbed dose to 50, 75, 100, 125, and 150 kGy. Based on data such as $E = 250$ keV, $I = 1$ mA, $s = 6$ cm, $L = 60$ cm, $\eta = 60\%$, $\rho_a = 0.00112$ g/cm³, $\rho_l = 0.913$ g/cm³, $t_a = 3$ cm, $t_w = 20$ μ m, $\rho_w = 4.6$ g/cm³, the effect of D and C could be obtained from equations (4), (8), (9), (11), and (12), as shown in Figure 6. Figure 6 shows that lower absorbed dose in the EBM correlated with greater RVNRL capacity. The specific value used for t_l was 0.0114 cm when obtaining data in Figures 4-6 under conditions such as $E = 250$ keV, $I = 1$ mA, $t_a = 3$ cm, and $D = 50$ kGy.

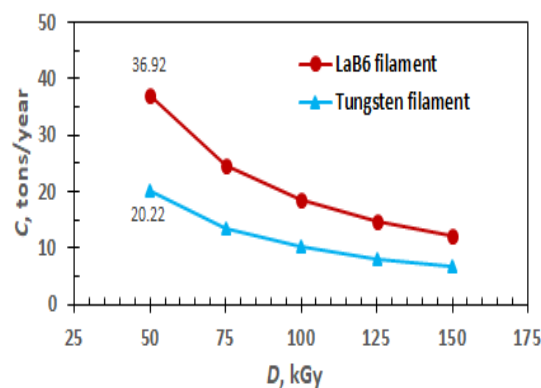


Figure 6 The effect of D and EBM filament materials on the C for EBM operates at $E = 250$ keV, $I = 1$ mA; and $t_a = 3$ cm

The results of empirical capacity calculations of RVNRL with tungsten or LaB₆ filament EBM are shown in Figures 4, 5, and 6. However, these results should be supported by the quality of experimental data of RVNRL such as crosslink density, tensile strength, elongation at break, and modulus of elasticity (Ahmed and Sabbagh, 2015; Ahsan et al., 2015; Junian et al., 2015; Soiket et al., 2015; Roslim et al., 2012). The initial design of 300 keV/20 mA EBM for RVNRL can be improved in performance to achieve operating conditions with $E > 250$ keV and $I > 1$ mA. This is achieved by

replacing several important tool components according to manufacturer standards to ensure safe operating conditions of EBM.

4. Conclusions

In conclusion, this study showed that RVNRL capacity for EBM under safe operating conditions of $E = 250$ keV and $I = 1$ mA, varied significantly based on filament. Using a tungsten filament with a lifetime of 30-100 hours, RVNRL capacity was $C = 20.22$ tons/year. Meanwhile, the selection of LaB6 as electron source produced 36.92 tons/year. These results provided valuable data input in determining the amount of EBM required to calculate capital expenditure for constructing RVNRL plant using EBM in Indonesia.

Acknowledgements

The authors gratefully acknowledges the Head of the Research Center for Accelerator Technology and the Head of the Research Center for Mining Technology, National Research and Innovation Agency (BRIN), for their support and for providing the opportunity to conduct this study.

Author Contributions

All authors contributed to the study conception and design. Data collection were performed by Suprpto S, Djoko SP, Samin S, Kris T.B. The first draft of the manuscript was written by Herry P, and Darsono D. Calculation and Simulation data were performed by Herry P, and Darsono D. All author contributed to data analysis and interpretation. Final manuscript were written by Suhadah R.A., Darsono D, and Herry P. All authors commented on previous versions of the manuscript.

Conflict of Interest

The authors declare that there is no conflict of Interest regarding the publication of this article.

References

- Ahmed, NM, & El-Sabbagh, SH 2015, 'The influence of doped-kaolin on the properties of styrene-butadiene rubber composites', *International Journal of Advanced Research*, vol. 3, no. 5, pp. 1-19
- Ahsan, Q, Mohamad, N, & Soh, TC 2015, 'Effects of accelerators on the cure characteristics and mechanical properties of natural rubber compounds', *International Journal of Automotive and Mechanical Engineering*, vol. 12, pp. 2954-2966, <https://doi.org/10.15282/ijame.12.2015.12.0247>
- Andler, R 2020, 'Bacterial and enzymatic degradation of poly(cis-1,4-isoprene) rubber: Novel biotechnological applications', *Biotechnology Advances*, vol. 44, article 107606, <https://doi.org/10.1016/j.biotechadv.2020.107606>
- Andrade, KL, Ramlow, H, Floriano, JF, Acosta, ED, Faixa, FL, & Machado, RAF 2022, 'Latex and natural rubber: recent advances for biomedical applications', *Polímeros: Ciência e Tecnologia*, vol. 32, no. 2, article e2022015, <https://doi.org/10.1590/0104-1428.20210114>
- Baudoin, M, Paboeuf, G, Liengprayoon, S, Musigamart, N, Bottier, C, & Vie, V 2025, 'Hevea brasiliensis rubber particles' fluid interfaces reveal size impact on early coagulation steps', *Colloids and Surfaces B: Biointerfaces*, vol. 245, article 114281, <https://doi.org/10.1016/j.colsurfb.2024.114281>
- Che, J, Burger, C, Toki, S, Rong, L, Hsiao, BS, Amnuaypornsi, S, & Sakdapipanich, J 2013, 'Crystal and crystallites structure of natural rubber and synthetic cis-1,4-polyisoprene by a new two dimensional wide angle X-ray diffraction simulation method. I. Strain-induced crystallization', *Macromolecules*, vol. 46, pp. 4520-4528, <https://doi.org/10.1021/ma400420k>
- Cifriadi, A, Chalid, M, & Puspitasari, S 2017, 'Characterization of hydrogenated natural rubber synthesized diimide transfer hydrogenation', *International Journal of Technology*, vol. 8, no. 3, pp. 448-457, <https://doi.org/10.14716/ijtech.v8i3.1991>
- Darsono 2009, 'Industrial scale MBE for production of irradiated natural rubber latex: Manufacturing, market share, and techno-economics of LKAI', *In: Proceedings of Scientific Meeting and Presentation of Accelerator Technology and Its Applications*, pp. 91-101

Darsono, Taufik, Suprpto, Saefurrochman, Elin, N, & Sutadi 2024, 'Construction and characterization of the diode and triode electron sources for EBM 300 keV/20 mA', *International Journal of Technology*, vol. 15, no. 1, pp. 154-165, <https://doi.org/10.14716/ijtech.v15i1.4406>

Electron Microscopy Sciences (EMS) 2023, *Cathodes & filaments for electron microscopes*, Electron Microscopy Sciences

Febriasari, A, Suhartini, M, Yunus, AL, Rahmawati, S, Hotimah, B, Hemana, RF, Kartohardjono, S, Fahira, A, & Permatasari, IP 2021, 'Gamma irradiation of cellulose acetate-polyethylene glycol 400 composite membrane and its performance test for gas separation', *International Journal of Technology*, vol. 12, no. 6, pp. 1198-1206, <https://doi.org/10.14716/ijtech.v12i6.5250>

Harahap, H, Hadinatan, K, Hartanto, A, Surya, E, & Surya, I 2015, 'Utilization of cassava peel waste modifies alkanolamide as filler in natural rubber latex products: The effect of drying time', *Magazine of Leather Rubber and Plastic*, vol. 31, no. 1, pp. 1-8

International Atomic Energy Agency (IAEA) 2010, *Use of mathematical modelling in electron beam processing: A guidebook*, IAEA Radiation Technology Series No. 1, International Atomic Energy Agency, Vienna

Junian, S, Makmud, MZH, & Sahari, J 2015, 'Natural rubber as electrical an insulator: A review', *Journal of Advanced Review on Scientific Research*, vol. 6, no. 1, pp. 28-41

Junkong, P, Cornish, K, & Ikeda, Y 2017, 'Characteristics of mechanical properties of sulphur cross-linked guayule and dandelion natural rubbers', *RSC Advances*, vol. 17, pp. 50739-50752, <https://doi.org/10.1039/C7RA08554K>

Kim, DY, Park, JW, Lee, DY, & Seo, KH 2020, 'Correlation between the crosslink characteristics and mechanical properties of natural rubber compound via accelerators and reinforcement', *Polymers*, vol. 12, no. 9, pp. 1-14, <https://doi.org/10.3390/polym12092020>

Kovalskiy, SS 2017, *Low-energy electron beam for medical and plasma chemistry applications*, Beam & Plasma Technologies LLC, Tomsk

Lehman, N, Tuljitrarn, A, Songtipya, L, Uthaipan, N, Sengloyluan, K, Johns, J, Nakaramontri, Y & Kalkornsurapranee, E 2022, 'Influence of Non-Rubber Components on the Properties of Unvulcanized Natural Rubber from Different Clones', *Polymers*, vol. 14, article 1759, <https://doi.org/10.3390/polym14091759>

Li, K, Ricker, K, Tsai, FC, Hsieh, CYJ, Osborne, G, Sun, M, Marder, ME, Elmore, S, Schmitz, R, & Sandy, MS 2021, 'Estimated cancer risks associated with nitrosamine contamination in commonly used medications', *International Journal of Environmental Research and Public Health*, vol. 18, article 9465, <https://doi.org/10.3390/ijerph18189465>

Li, Y & Hecht, SS 2022, 'Metabolic activation and DNA interaction of carcinogenic N-nitrosamines to which humans are commonly exposed', *International Journal of Molecular Sciences*, vol. 23, no. 9, article 4559 <https://doi.org/10.3390/ijms23094559>

Lönartz, MI, McCoy, VE, Gee, CT, & Geisler, T 2023, 'Palaeoenvironmental conditions for the natural vulcanization of the Eocene "Monkeyhair" laticifers from Geiseltal, Germany, as elucidated by Raman spectroscopy', *Palaeobiodiversity and Palaeoenvironments*, vol. 103, pp. 681-693, <https://doi.org/10.1007/s12549-022-00566-8>

Marsongko 2013, 'Comparison of glove manufacture from radiation vulcanized natural latex and sulfur', *Jurnal Kimia dan Kemasan*, vol. 35, no. 2, pp. 131-136

Muktaridha, O, Adlim, M, Suhendrayatna, Ismail, & Abu Bakar, NHH 2021, 'Photocatalytic degradation of skim-latex-vapor odor using iron-doped zinc oxide', *International Journal of Technology*, vol. 12, no. 4, pp. 739-748, <https://doi.org/10.14716/ijtech.v12i4.4227>

Poernomo, H, & Saptaji, R 2012, 'Basic design of natural rubber latex vulcanization system with electron beams on a belt conveyor', *Proceedings of Scientific Meetings and Presentations-Basic Research on Nuclear Science and Technology*, pp. 102-107

Radford, R, Frain, H, Ryan, MP, Slattery, C, & McMorro, T 2013, 'Mechanisms of chemical carcinogenesis in the kidneys', *International Journal of Molecular Sciences*, vol. 14, no. 10, pp. 19416-19433, <https://doi.org/10.3390/ijms141019416>

Roslim, R, Hashim, MYA, & Augurio, PT 2012, 'Natural latex foam', *Journal of Engineering Science*, vol. 8, pp. 15-27

Samin, S, Suyanti, S, Sunanti, ST, & Adi, WA 2020, 'Synthesis and certification of lanthanum oxide extracted from monazite sand', *Indonesian Journal of Chemistry*, vol. 20, no. 6, pp. 1213-1220, <https://doi.org/10.22146/ijc.44327>

Saptaaji, R 2008, 'Determination of the depth of penetration of the 800 keV electron beam in the exhaust gas of a power plant in an exhaust gas treatment system using an electron beam machine', *Nuclear Forum Journal*, vol. 2, no. 1, pp. 51-62

Singh, G, Mahajan, A, & Kumar, M 2015, 'A review paper on vulcanization of rubber and its properties', *Global Journal of Engineering Science and Research*, vol. 2, no. 8, pp. 1-4

Soiket, MIH, Rana, MRA, & Al Ratun, J 2015, 'Experimental investigation on mechanical properties of indigenous rubber products', *American International Journal of Research in Science, Technology, Engineering & Mathematics*, vol. 15, pp. 139-142

Sukaryono 2021, *Safety analysis report of a 300 keV/20 mA electron beam machine*, Research Center for Accelerator Technology, Research Organization for Nuclear Energy, National Research and Innovation Agency, Indonesia

Suprpto, & Djoko, SP 2007, 'Design of irradiation vessel for vulcanization of natural rubber latex using electron beam irradiation', *In: Proceedings of Technology Scientific Meeting and Presentation Accelerators and Their Applications*, pp. 27-35

Tosaka, M, Kawakami, D, Senoo, K, Kohjiya, S, Ikeda, Y, Toki, S, & Hsiao, BS 2006, 'Crystallization and stress relaxation in highly stretched samples of natural rubber and its synthetic analogue', *Macromolecules*, vol. 39, pp. 5100-5105, <https://doi.org/10.1021/ma060407>

Trabelsi, S, Albouy, PA, & Rault, J 2004, 'Stress-induced crystallization properties of natural and synthetic cis-polyisoprene', *Rubber Chemistry and Technology*, vol. 77, pp. 303-316, <https://doi.org/10.5254/1.3547825>

Trisnawati, I, Prameswara, G, Mulyono, P, Prasetya, A, & Petrus, HTBM 2020, 'Sulfuric acid leaching of heavy rare earth elements (HREEs) from Indonesian zircon tailing', *International Journal of Technology*, vol. 11, no. 4, pp. 804-816, <https://doi.org/10.14716/ijtech.v11i4.4037>

Widiyati, C, & Poernomo, H 2018, 'Design of a prototype photoreactor UV-LEDs for radiation vulcanization of natural rubber latex', *International Journal of Technology*, vol. 9, no. 1, pp. 130-141, <https://doi.org/10.14716/ijtech.v9i1.1164>

Widiyati, C, & Poernomo, H 2022, 'Comparison of technology of radiation vulcanized natural rubber latex using UV-mercury lamp, UV-LED lamp, and plasma cathode-based EBM irradiators', *Jurnal Teknologi (Sciences & Engineering)*, vol. 84, no. 3, pp. 111-123, <https://doi.org/10.11113/jurnalteknologi.v84.17507>

Yamano, M, Yamamoto, Y, Saito, T & Kawahara, S 2021, 'Preparation and characterization of vulcanized natural rubber with high stereoregularity', *Polymer*, vol. 235, article 124271, <https://doi.org/10.1016/j.polymer.2021.124271>